

# Magnetic field dependent thermosolutal convection flow between two squeezing plates

## Abstract

The effect of magnetic field dependent thermosolutal convection and MFD viscosity of the fluid dynamic are studied between two squeezing plates. The unsteady constitutive expression of mass conservation modified Navier-Stokes, Maxwell and MFD thermosolutal convection are coupled as a system of ordinary differential equations. The corresponding solution for momentum as well as solution for the magnetic field equations are determined by the PCM method. The validity and accuracy of PCM results is proved by the comparison of the PCM solution with numerical solver package BVP4c. It has been shown the magnetic Reynold number caused to decrease the flow, magnetic field distribution and temperature of the fluid. Also x-component and y- component of magnetic field have opposite behavior with increase in MFD viscosity.

## Nomenclature

$p$	pressure	$C$	dimensional concentration
$x, y, z$	Cartesian coordinate	$\kappa$	thermal conductivity
$U_x$	x-component of velocity( $m. s^{-1}$ )	$\mu$	dynamic viscosity
$U_y$	y-component of velocity( $m. s^{-1}$ )	$\nu$	kinematic viscosity
$U_z$	z-component of velocity( $m. s^{-1}$ )	$\sigma$	electrical conductivity
$t$	time(s)	$\rho$	fluid density
$T_u$	temperature at upper plate( $k$ )	$\alpha$	positive constant
$T_l$	temperature at lower plate( $k$ )	$\eta$	similarity variable
$C_u$	concentration at upper plate	$\theta$	dimensionless variable
$C_l$	concentration at lower plate	$\varphi$	dimensionless variable
$p_r$	prandtl number( $\nu/k$ )	'	derivative w.r.t $\eta$
$N_b$	squeezing parameter	*	dimensionless variable
$D(t)$	distance between two plates	$u$	fluid condition on upper plate
$c_p$	specific heat of fluid( $J/kgk$ )	$l$	fluid condition on upper plate
$H_m$	Hartmann number	$U$	fluid velocity( $m. s^{-1}$ )
$E_c$	Eckert number	$T$	fluid temperature
$m_\eta$	magnetic field dependent viscosity	$P_m$	pyromagnetic coefficient
$N_{em}$	magnetic Reynold number	$P_s$	salinity magnetic coefficient
$N_c$	strength of magnetic field		

## Introduction

Research based studies show that magnetic fields can reduce the heart attack risk by streamlining the blood flow. Tao and Huang showed that when magnetic field is applied parallel to blood direction, it

significantly reduced blood viscosity. This processes widely used in engineering (fluid film in power transmission, hydro magnetic lubrication of breaking devices and pistons system in engines). Ferro hydrodynamics (FHD) is mechanics of fluid motion under magnetic polarization. Magnetic fluids are involved in heat transfer processes via Ferro fluids. Liquid cooled are example of such processes, in which Ferro fluids carry heat away from coils. [1]. This invention increases the coil's amplifying capacity, which contributes to high fidelity sound generation in loud speakers. Another crucial application of magnetic field is in the field of drug designing where magnetic field is used to carry drug to desired target sites in the human body, a drop of Ferro fluid in human body can be detected by the magnetic field [2]. According to Lenz's law when conducting fluid move in magnetic field then magnetic field changes its motion. In MHD, the motion changes the field and vice versa [3, 4]. Alloys have important applications in heat transfer processes such a steel, brass and bronze are few typical examples. Alloys have applications in various fields including powder technology, aerospace technology and in surgeries. Recently Aamir et al. [5] studied the Theremosolutal convection between coaxial contracting disc and investigated the fluid dynamic aspects of these magnetic field dependent discs. They studied their problem in cylindrical coordinate system and analyzed the flow field, temperature variation, skin fraction and Nusselt number.

### Literature Review

The study of squeezing flow has it origin in the 19<sup>th</sup> century and continues to receive considerable attention due to practical application in physical and biophysical area. Stoke problems of a convective flow past a perpendicular infinite plates in a spinning systems in occurrence of inconsistent magmatic field was studied by Mutua et al. [6]. He concluded that velocity field and temperature depend upon all of the parameters. The effect of these parameters changes the rate of heat transfer as well as the skin friction. It was observed that that increasing magnetic parameter ( $M$ ) and Eckert number ( $Ec$ ) elevated the free convection heating and as free convection cooling velocity profile. Seth [7] examined heat transfer and MHD flow on a porous flat plate along with mass transfer. Fluid velocity component was observed to be raised as the Hall parameter and value of time was increased. Unsteady flow between two permeable squeezed plates with thermal radiation has been studied by Victor [8]. For analysis he used Galerkin finite element method. He concluded that the fluid velocity and temperature distribution are strongly depended on Radiation parameter and on Prandle number. In his study he also concluded that Grashof number and Magnetic parameter have a negligible effect on temperature distribution. Inclined magnetic field applied on coutee flow inside two parallel porous plates. was studied by Simon [9]. He considered the lower plate is absorbent and motionless. He found that fluid velocity decrease with a rise in magnetic field. For the solution of the magnetic squeeze film problem Rashidi et al. [10] used the DTM-Pade combined method to determine convergence, stability and versatility. The important effect of changing the electrical conductivity of a viscous, incompressible and electrically conducting fluid on the free convection flow was observed. Furthermore, it was noted that heat transfer on the isothermal non conducting plate was also influenced by changing the electrical conductivity. Shorma et al. [11] Studied natural convection flow and heat generation in electrically conductivity flow. It was reported that suitable magnetic field can change aerodynamic force along with heat transfer rates in convenient manner. This type of MHD studies are linked with fission reactor development where the plasma is restricted by use of strong magnetic field [12]. MHD effects in the so-called blanket was studied by Morley [13]. The blanket is present between the magnetic field coils and plasma. Blanket is used for the avoiding radiation damages. Sohail et al [14]. explored the way in which flow between two squeezing plates is effecting by changing the magnetic field Recently aamir et al. [15] studied the theremosolutl convection between coaxial contracting disc and investigated the fluid dynamic aspects of these magnetic field dependent discs. They studied their problem is cylindrical coordinate system then analyzed the flow field, temperature variation, skin fraction and nusselt number. Nath and murugesan investigatate[16] the influence of nano particles shape on heat and mass transport phenomena

in a moving lid cavity under the combined effect of thermosolutal buoyancy force and magnetic force. The diffusion moved of transport processes is stronger than the convection mode at higher inclination angle of magnetic field. Nusselt and Sherwood number respectively except the platelet shape that shows that maximum fractional loss in term of wall shear stress. The dynamical model follows the usual conservation laws and is reduced through a nonsimilar group of transformations. The resulting equations are solved using a spectral-based local linearization method, and the accuracy of the numerical results is validated through the grid dependence and convergence tests. Detailed analyses of the effects of specific thermophysical parameters are presented through tables and graphs. The study reveals, among other results, that the buoyancy force, solute and thermal expansion coefficients, and thermal radiation increase the overall wall drag, heat, and mass fluxes [17] studied by Tijani.

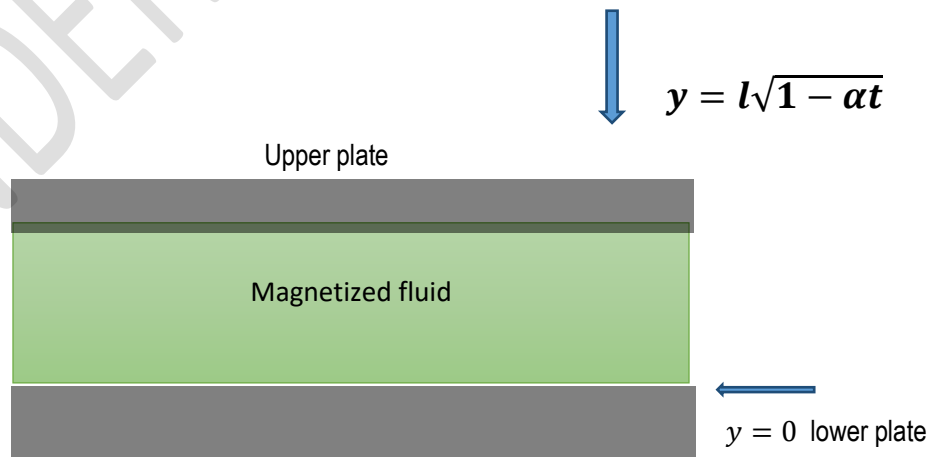
### Problems formulation

Suppose that an incompressible and axisymmetric viscous fluid divided by the distance of  $y = l\sqrt{1 - \alpha t}$  between two parallel squeezing plates, where  $l$  is length equal to the separation of plates at  $t=0$ . For  $\alpha > 0$  both plates are pressed until they reach at  $t = \frac{1}{\alpha}$  both are separated at  $\alpha < 0$ . Lower plate is stationary and upper plate are squeeze it is considered to be the optimal conductor for both surfaces, according to Hughes. The electrical forces are much smaller than the magnetic forces and consequently are ignored in the present problem. The applied magnetic field produced to induced magnetic field  $(B_x, B_y, B_z)$

$$H_x = \frac{\alpha x E_0}{(\mu_2(1 - \alpha t))} \quad H_y = \frac{-x E_0}{\mu_1(1 - \alpha t)^{0.5}} \quad H_z = \frac{x F_0}{\mu_2(1 - \alpha t)}$$

$E_0$  and  $F_0$  are dimensionless  $\mu_1$  and  $\mu_2$  are the external and inner media magnetic permeability between the two plates, respectively. Incompressible fluid is presumed to have a variable viscosity given by  $\mu = \mu_0(1 + \partial \cdot B)$  in the absence of the magnetic field  $\mu_0$  is the viscosity of the fluid.  $\partial_x = \partial_y = \partial_z$  isotropic was taken for the variance coefficient of viscosity  $\partial$ . The component of the  $\mu$  are  $\mu_x = \mu_0(1 + \partial B_x)$ ,  $\mu_y = \mu_0(1 + \partial B_y)$  and  $\mu_z = \mu_0(1 + \partial B_z)$  further  $B = \mu_p(M + H)$  where  $M$  is magnetization  $H$  is magnetic field and  $\mu_p$  is magnetic permeability. The effect of shear viscosity dependency is not taken into account since it has a marginal effect on a high field mono dispersive device. The equations governing viscous fluid flow and heat transfer are:

### Geometry of problem



### 3.2 Basic governing equations

Continuity equation

$$\nabla \cdot U = 0 \quad (1)$$

Maxwell equation

$$\nabla \cdot B = 0, \quad \nabla \times B = 0 \quad (2)$$

Navier stoke equation

$$\rho \left[ \frac{\partial U}{\partial t} + (U \cdot \nabla)U \right] + \nabla p - \mu \nabla^2 U - \frac{1}{\mu_2} (\nabla \times B) \times B = 0 \quad (3)$$

Magnetic field equation

$$\frac{\partial B}{\partial t} - \nabla \times (U \times B) - \frac{1}{\sigma \mu_2} \nabla^2 B = 0 \quad (4)$$

Solute concentration equation is

$$[\rho_0 C_{s,h} - \mu_0 H \cdot \left( \frac{\partial M}{\partial T} \right)] \frac{DT}{Dt} + \mu_0 T \left( \frac{\partial M}{\partial T} \right) \frac{DH}{Dt} = K_1 \nabla^2 T \quad (5)$$

Solute concentration

$$[\rho_0 C_{s,h} - \mu_0 H \cdot \left( \frac{\partial M}{\partial C} \right)] \frac{DC}{Dt} + \mu_0 C \left( \frac{\partial M}{\partial C} \right) \frac{DH}{Dt} = K'_1 \nabla^2 C \quad (6)$$

U is fluid velocity,  $\sigma$  is electrical conductivity,  $\rho_0$  is reference density,  $\rho$  is the density of fluid, p is pressure of fluid,  $\mu$  is variable dynamic viscosity,  $C_{s,h}$  is specific heat of constant volume, T is temperature, C is solute concentration, M is magnetization,  $K_l$  is thermal conductivity,  $K'_l$  solute conductivity.

Boundary condition are chosen as:

$$U_x = 0, U_y = 0, U_z = \frac{\sigma_1 x}{1 - \alpha t}, B_x = 0, B_y = 0, B_z = 0.$$

$$T = T_l, C = C_l \text{ at } Y = 0.$$

$$U_x = 0, U_y = \frac{-\alpha l}{2\sqrt{1 - \alpha t}}, U_z = \frac{\sigma_u x}{1 - \alpha t}.$$

$$B_x = 0, B_y = \frac{-xE_0}{\sqrt{1 - \alpha t}}, B_z = \frac{xF_0}{1 - \alpha t}.$$

$$T = T_u, C = C_u \text{ at } y = l\sqrt{1 - \alpha t}. \quad (7)$$

Where  $U_x, U_y, U_z$  are respectively the x, y and z component of the velocity,  $\alpha, T_l$  and  $C_l$  represent the thermal diffusivity temperature at lower plate and concentration at lower plate are respectively, while temperature and concentration at upper plate are represent by  $T_u, C_u$  respectively,  $c_p$  specific heat at constant pressure. Introducing the following similarity transformation are chosen for reducing the partial differential equations (1) to (6) to a system of ordinary differential equations.

$$U_x = \frac{\alpha x}{2(1 - \alpha t)} m(\eta), \quad U_y = \frac{-\alpha l}{\sqrt{1 - \alpha t}} m(\eta),$$

$$U_z = \frac{\sigma_1 x}{1 - \alpha t} n(\eta), \quad B_x = \frac{\alpha x E_0}{2L^2(1 - \alpha t)} h(\eta),$$

$$, B_y = \frac{-aE_0}{l\sqrt{1-at}} h(\eta) \quad , B_z = \frac{2vx F_0}{al(1-at)} k(\eta)$$

$$\theta = \frac{T-T_u}{T_l-T_u}, \quad \varphi = \frac{c-c_u}{c_l-c_u}, \quad \eta = \frac{y}{l\sqrt{1-at}} . \quad (8)$$

The partial differential equations (3.1) to (3.6) are transform in the form of following ordinary differential equations.

$$m'''' = \frac{N_b}{m_\eta} [2m'' + \eta m'''' - 2mm'' + 2N_c^2 N_{em} (2hh' + \eta hh'' + 2h^2 m'' - 2hmh'')]. \quad (9)$$

$$n'' = \frac{1}{m_\eta} [N_b (2n + \eta n' + m'n - 2mn') - N_c N_d (h'k - 2hk')]. \quad (10)$$

$$h'' = N_{em} (h + \eta h' + hm' - mh'). \quad (11)$$

$$k'' = N_{em} (2k + \eta k' - 2mk') + \frac{N_c N_{em}}{N_d} (hn'). \quad (12)$$

$$\theta'' = N_b P_r (\eta \theta' - 2m\theta') - P_m \nabla T H_m E_c (2(\eta h\theta' - 2mh\theta') + (h\theta + \eta h'\theta - 2mh'\theta')). \quad (13)$$

$$\varphi'' = N_b P_r (\eta \varphi' - 2m\varphi') - P_c \nabla T H_m E_c (2(\eta h\varphi' - 2mh\varphi') + (h\varphi + \eta h'\varphi - 2mh'\varphi')). \quad (14)$$

Boundary condition are reduced to

$$m(0) = 0, m'(0) = 0, n(0) = 1, \theta(0) = 1, \varphi(0) = 1, h(0) = 0, k(0) = 0,$$

$$m(1) = 0.5, m'(1) = 0, n(1) = 1, \theta(1) = 0, \varphi(1) = 0, h(1) = 1, k(1) = 1. \quad (15)$$

Where  $N_b$  is rotational Reynold number,  $N_{em}$  is magnetic Reynold number  $N_c$  is strength of magnetic field in y direction  $N_d$  strength of magnetic field in z direction,  $m_\eta$  is magnetic field dependent viscosity parameter.  $P_r, E_c, H_m, P_m, P_s$  are Prandtl number Eckert number Hartman number pyro magnetic coefficient and salinity magnetic coefficient are respectively.

After solving these equations by PCM methods and BVP4C methods we get a different table and graph are

$\eta$	Numerical results					PCM results				
	$m(\eta)$	$n(\eta)$	$h(\eta)$	$\theta(\eta)$	$\varphi(\eta)$	$m(\eta)$	$n(\eta)$	$h(\eta)$	$\theta(\eta)$	$\varphi(\eta)$
.1	0.0143	0.9171	0.9000	0.9063	0.9157	0.0141	0.9170	0.900	0.9066	0.9157
.2	0.0525	0.8411	0.1805	0.8121	0.8308	0.0522	0.8411	0.1805	0.8127	0.8308
.3	0.1087	0.7725	0.2722	0.7170	0.7452	0.1083	0.7724	0.2722	0.7179	0.7452
.4	0.1767	0.7112	0.3659	0.6190	0.6568	0.1762	0.7112	0.3659	0.6198	0.6568
.5	0.2508	0.6575	0.4620	0.5234	0.5705	0.2500	0.6575	0.4620	0.5237	0.5705
.6	0.3247	0.6113	0.5613	0.4241	0.4805	0.3240	0.6112	0.5613	0.4249	0.4805
.7	0.3926	0.5725	0.6644	0.3227	0.3881	0.3920	0.5724	0.6644	0.3232	0.3881
.8	0.4485	0.5411	0.7716	0.2186	0.2923	0.4480	0.5410	0.7716	0.2180	0.2923
.9	0.4863	0.5170	0.8834	0.1112	0.1920	0.4860	0.5170	0.8834	0.1119	0.1920

TABLE.1: Computation for  $m(\eta), n(\eta), h(\eta), k(\eta), \theta(\eta)$  with  $N_b = 0.1, N_c = 0.2, N_d = 0.5, P_r = 0.2, H_m = 1, P_m = 0.2, P_s = 1, N_{em} = 0.3, E_c = 2, S=1, m_\eta=0.3$  and various values of  $\eta$ .

$m_\eta$	Numerical results			PCM results		
	$m''(0)$	$-n'(0)$	$-\theta'(0)$	$m''(0)$	$-n'(0)$	$-\theta'(0)$
1	3.0232	0.2524	1.1545	3.0172	0.2521	1.1554

2	3.0146	0.1292	1.1545	3.0086	0.1291	1.1554
3	3.0117	0.869	1.1545	3.0057	0.0867	1.1554
4	3.0103	0.0654	1.1545	3.0043	0.0653	1.1554

TABLE.2:Computation for  $m''(\eta)$ ,  $-n'(\eta)$ ,  $-h'(\eta)$ ,  $-k'(\eta)$ ,  $-\theta'(\eta)$  with  $N_b = 0.2, N_c = 0.1, N_d = 1, P_r = 2, H_m = 1, P_m = 1, P_s = 0.5, N_{em} = 0.5, E_c = 2, S=1$  and various of  $m_\eta$

$N_{em}$	Numerical results			PCM results		
	$m''(0)$	$-n'(0)$	$-\theta'(0)$	$m''(0)$	$-n'(0)$	$-\theta'(0)$
.5	3.0117	0.0869	1.1545	3.0057	0.0867	1.1554
1	3.0118	0.0863	1.1334	3.0058	0.0863	1.1342
2	3.0118	0.0853	1.1000	3.0058	0.0853	1.1005
3	3.0118	0.0846	1.0751	3.0058	0.0847	1.0756

TABLE.3:Computation for  $m''(\eta)$ ,  $-n'(\eta)$ ,  $-h'(\eta)$ ,  $-k'(\eta)$ ,  $-\theta'(\eta)$  with  $N_b = 0.2, N_c = 0.1, N_d = 1, P_r = 2, H_m = 1, P_m = 0.2, P_s = 0.5, E_c = 2, m_\eta = 3, S=1$  and various values of  $N_{em}$ .

$E_c$	Numerical results			PCM results		
	$m''(0)$	$-n'(0)$	$-\theta'(0)$	$m''(0)$	$-n'(0)$	$-\theta'(0)$
0.1	3.0127	0.1421	1.0015	3.0068	0.1421	1.0015
0.5	3.0127	0.1421	1.0087	3.0068	0.1421	1.0088
1	3.0127	0.1421	1.0176	3.0068	0.1421	1.0178
1.5	3.0127	0.1421	1.0265	3.0068	0.1421	1.0268

TABLE.4:Computation for  $m''(\eta)$ ,  $-n'(\eta)$ ,  $-h'(\eta)$ ,  $-k'(\eta)$ ,  $-\theta'(\eta)$  with  $N_b = 0.1, N_c = 2, N_d = 1, P_r = 0.2, H_m = 1, P_m = 0.2, P_s = 1, N_{em} = .3, m_\eta = 3, S=1$  and various values of  $E_c$ .

Pm	Numerical results			PCM results		
	$m''(0)$	$-n'(0)$	$-\theta'(0)$	$m''(0)$	$-n'(0)$	$-\theta'(0)$
0.1	3.0188	0.1241	1.0114	3.0148	0.1249	1.0114
0.5	3.0188	0.1241	1.0684	3.0148	0.1249	1.0688
1	3.0188	0.1241	1.1370	3.0148	0.1249	1.1377
1.5	3.0188	0.1241	1.2023	3.0148	0.1249	1.2029

TABLE.5:Shows  $n(\eta)$  and  $k(\eta)$  with various values of  $N_d$  and constant values of  $N_b = 0.1, N_c = 5, N_{em} = 1, P_r = 1, H_m = 10, P_m = 1, P_s = 1, m_\eta = 2, E_c = 0.1$

Ps	Numerical results			PCM results		
	$m''(0)$	$-n'(0)$	$-\varphi'(0)$	$m''(0)$	$-n'(0)$	$-\varphi'(0)$
.1	3.0188	0.1241	1.0116	3.0148	0.1249	1.0114
.5	3.0188	0.1241	1.0672	3.0148	0.1249	1.0688
1	3.0188	0.1241	1.1296	3.0148	0.1249	1.1377
1.5	3.0188	0.1241	1.1854	3.0148	0.1249	1.1998

TABLE.6:Computation for  $m''(\eta)$ ,  $-n'(\eta)$ ,  $-h'(\eta)$ ,  $-k'(\eta)$ ,  $-\theta'(\eta)$  with  $N_b = 0.2, N_c = 0.1, P_r = 2, H_m = 1, E_c = 2, m_\eta=3, P_m=.5, N_{em}=1, S=1$  and various values of  $P_s$ .

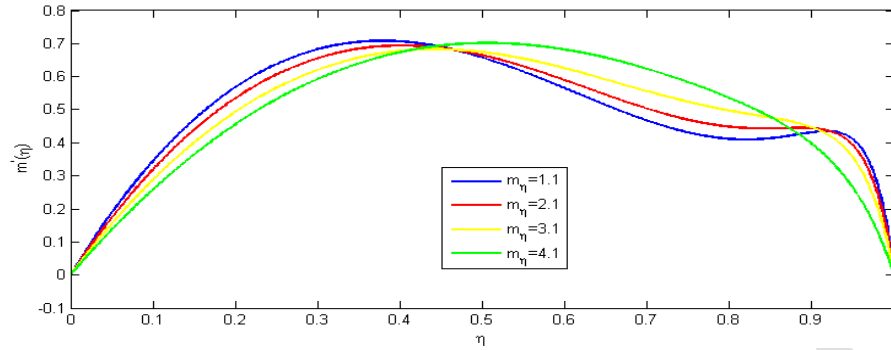


Figure 1a: Shows the effect of  $m'(\eta)$ , for various values of  $m_\eta$  and constant values of  $N_b = 0.2, N_c = 8, N_d = 1, P_r = 2, H_m = 1, P_m = 9, P_s = 1, N_{em} = 13, E_c = 0.3$ .

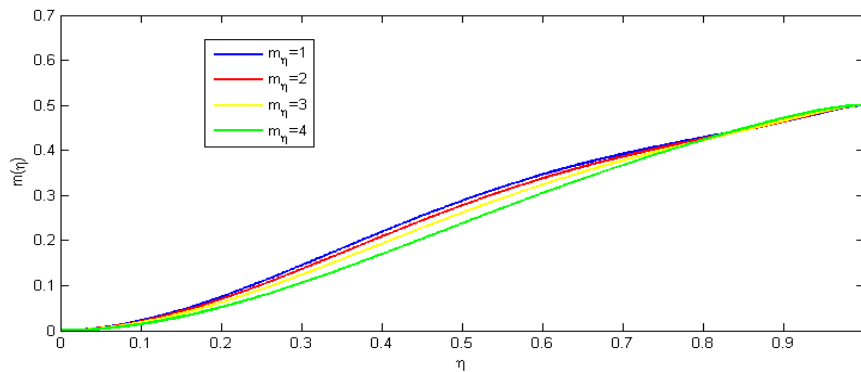


Figure 1b: Shows the effect of  $m(\eta)$ , for various values of  $m_\eta$  and constant values of  $N_b = 0.2, N_c = 8, N_d = 1, P_r = 2, H_m = 1, P_m = 9, P_s = 1, N_{em} = 13, E_c = 0.3$ .

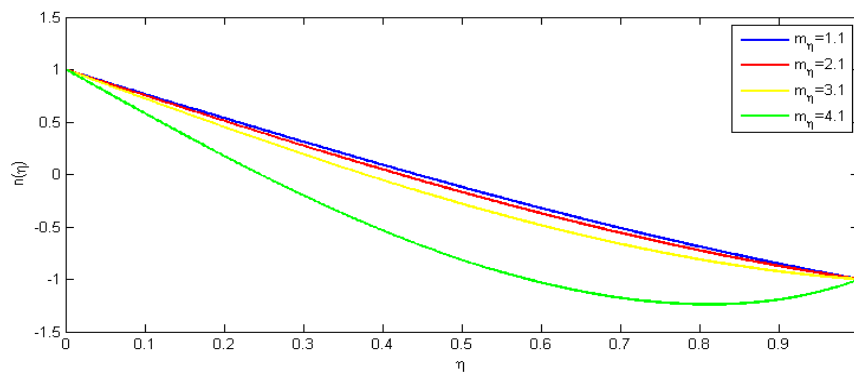


Figure 2b: Shows the  $k(\eta)$  with various values of  $m_\eta$  and constant values of  $N_b = .01, N_c = 3, N_d = 2, P_r = .2, H_m = 1, P_m = 1, P_s = .5, N_{em} = 0.5, E_c = 0.3$ ,

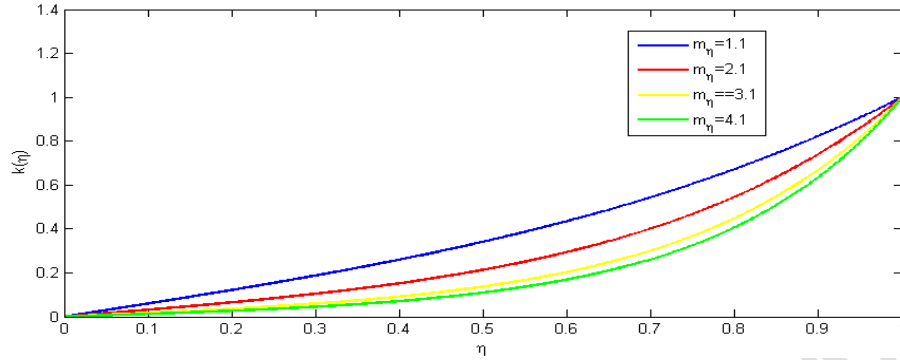


Figure 2c: Shows the  $k(\eta)$  various values of  $m_\eta$  and constant values of  $N_b = .01, N_c = 3, N_d = 2, P_r = .2, H_m = 1, P_m = 1, P_s = .5, N_{em} = 0.5, E_c = 0.3$ .

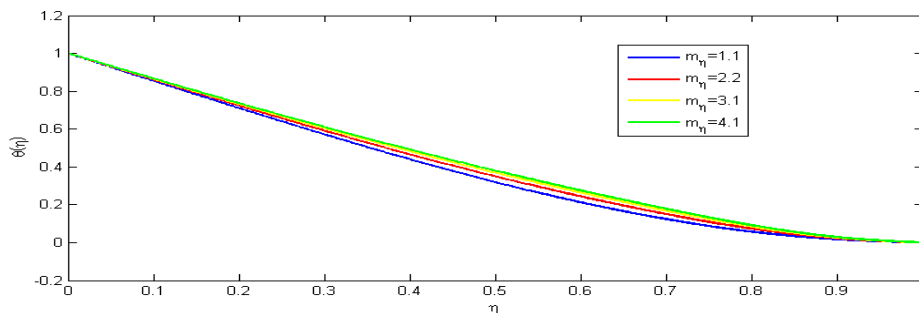


Figure 2d: Shows the  $\theta(\eta)$ , various values of  $m_\eta$  and constant values of  $N_b = .01, N_c = 3, N_d = 2, P_r = .2, H_m = 1, P_m = 1, P_s = .5, N_{em} = 0.5, E_c = 0.3$ .

### Results and discussion

The effect of MFDV  $m_\eta$  on  $m(\eta)$  and  $m'(\eta)$  can be seen in Figure 1. The resistance force of fluid flow increases as the viscosity coefficient rises as a result flow velocity decreases. Figure 1b indicates that as the viscosity of a fluid increases, the fluid flow at the center of the channel decreases that reflect the viscosity function as defined. As the viscosity parameter rises the fluid internal resistance increases as a result the flow decreases. It was also discovered that the fluid flow in the x direction decreases near the lower plate due to inertia and in the central zone it increases and start gradually decrease as it approaches the upper plates. Figure 2(a) shows the largest reduction in the z-component of velocity  $n(\eta)$  near the upper plate for a fixed value of  $m_\eta = 4$ , while for other various values of  $m_\eta$ ,  $h(\eta)$  and  $k(\eta)$  have the



opposite

behavior.

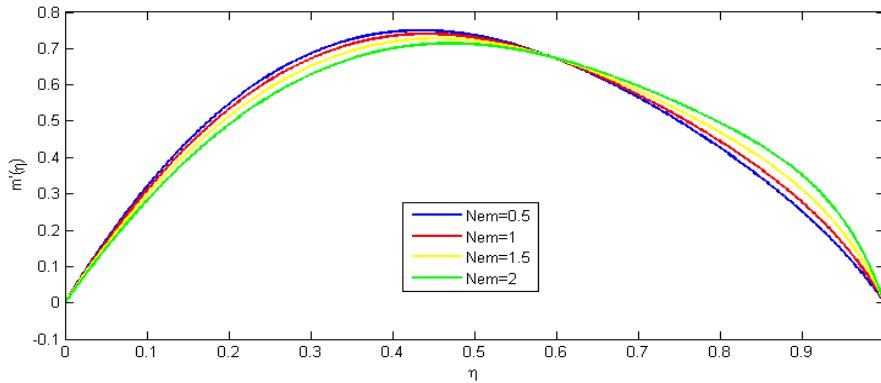


Figure 3 a: Shows the effect of  $m'(\eta)$ , at the various values of  $N_{em}$  and constant values of  $N_b = 0.9, N_c = 10, N_d = 0.2, P_r = 0.2, H_m = 1, P_m = 1, P_s = 0.5, m_\eta = 3, E_c = 5$ .

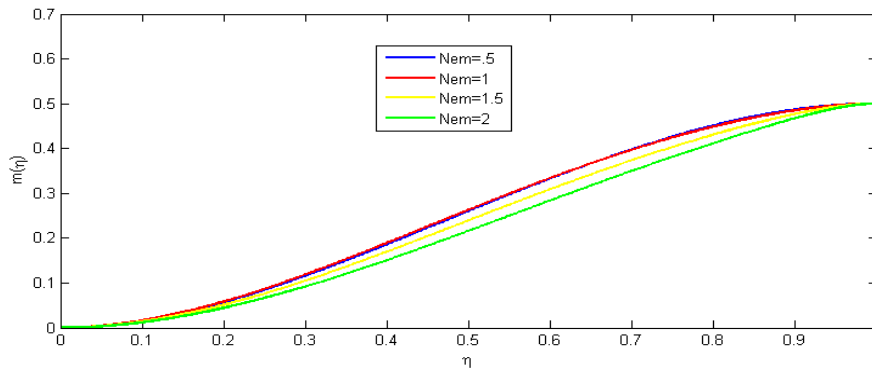


Figure 3 b: Shows the effect of  $m(\eta)$  at the various values of  $N_{em}$  and constant values of  $N_b = 0.9, N_c = 10, N_d = 0.2, P_r = 0.2, H_m = 1, P_m = 1, P_s = 0.5, m_\eta = 3, E_c = 5$ .

Figure 3 shows the effect of magnetic Reynold number on velocity component of  $m(\eta)$  and  $m'(\eta)$  Figure 3a indicates that as the magnetic Reynold's number increases the velocity component in x-direction decreases in the surrounding of lower plate while it increases near the region of upper plate. This is because the magnetic Reynold number depends upon the squeezing of upper plate as the upper plate moves away from lower plate the ratio of fluid flux to magnetic diffusivity increases and as a result the velocity of fluid increase from central region to upper plate. Similarly opposite behavior can be seen in figure 3b where the y-component of velocity increases and its value is maximum is achieved at  $N_{em}=2$  for the specific values of other parameters.

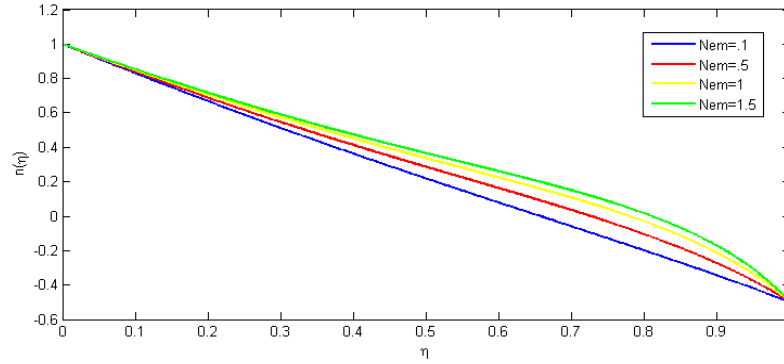


Figure 4(a): shows the effect of  $n(\eta)$ , with various values of  $N_{em}$  and at constant values of  $N_b = 0.9, N_c = 8, N_d = 0.2, P_r = 0.2, H_m = 10, P_m = 1, P_s = .5, m_\eta = 3, E_c = 5$ .

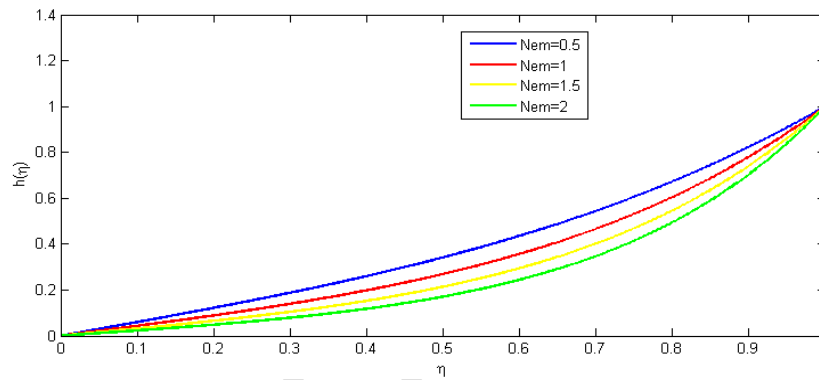


Figure 4(b): shows the effect of  $h(\eta)$  with various values of  $N_{em}$  and at constant values of  $N_b = 0.9, N_c = 8, N_d = 0.2, P_r = 0.2, H_m = 10, P_m = 1, P_s = .5, m_\eta = 3, E_c = 5$ .

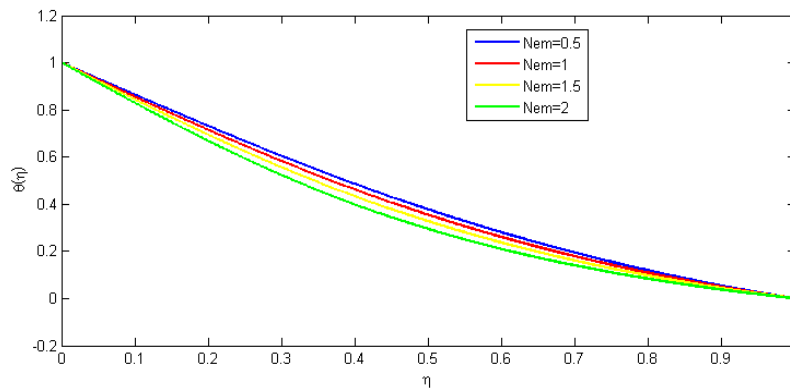


Figure 4(c): shows the effect of  $\varphi(\eta)$ , with various values of  $N_{em}$  and at constant values of  $N_b = 0.9, N_c = 8, N_d = 0.2, P_r = 0.2, H_m = 10, P_m = 1, P_s = .5, m_\eta = 3, E_c = 5$ .

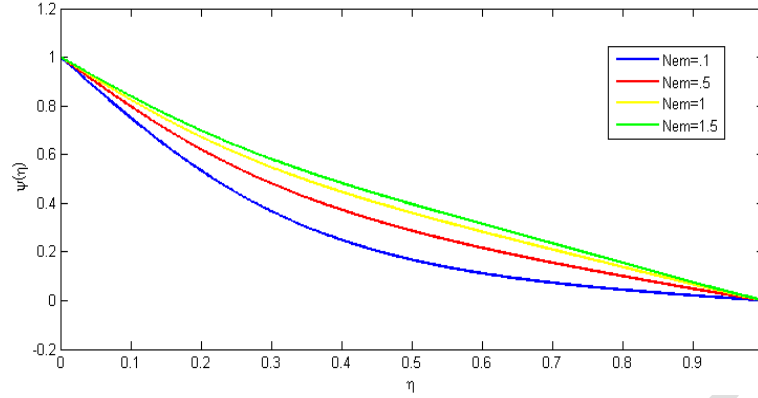


Figure 4d: Shows the effect  $\varphi(\eta)$ , with various values of  $N_{em}$  and at constant values of  $N_b = 0.9, N_c = 8, N_d = 0.2, P_r = 0.2, H_m = 10, P_m = 1, P_s = .5, m_\eta = 3, E_c = 5$ .

Figure 4a show the effect of magnetic Reynold number on z-component of velocity. From this figure one can observe that on increasing the magnetic Reynold number the z-component of velocity rises. It also observed that on increasing magnetic flux or decreasing diffusivity  $h(\eta), \theta(\eta)$  and  $\varphi(\eta)$  shows same behavior as shown in figure 4(b-d) and clear increases are observed in  $\theta(\eta)$  and  $\varphi(\eta)$ .

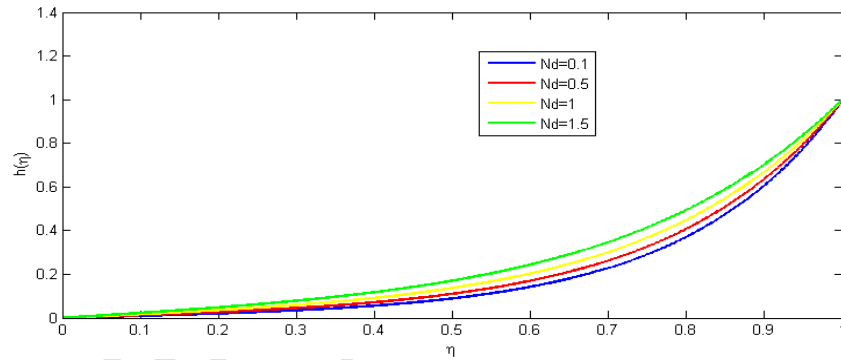


Figure 5a: Shows  $h(\eta)$  and  $k(\eta)$  with various values of  $N_d$  and constant values of  $N_b = 0.1, N_c = 5, N_{em} = 1, P_r = 1, H_m = 10, P_m = 1, P_s = 1, m_\eta = 2, E_c = 0.1$ .

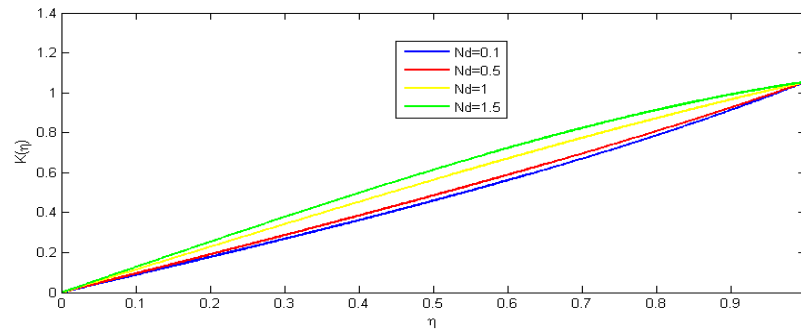


Figure 5b: Shows  $h(\eta)$  and  $k(\eta)$  with various values of  $N_d$  and constant values of  $N_b = 0.1, N_c = 5, N_{em} = 1, P_r = 1, H_m = 10, P_m = 1, P_s = 1, m_\eta = 2, E_c = 0.1$ .

Figure 5 shows the effect of  $N_d$  on magnetic component in y-direction i.e.  $h(\eta)$  and on magnetic component in z-direction i.e.  $k(\eta)$ . As  $N_d$  shows the strength of applied magnetic field along the z axis, so on increasing  $N_d$  the magnetic field in z-direction increases.

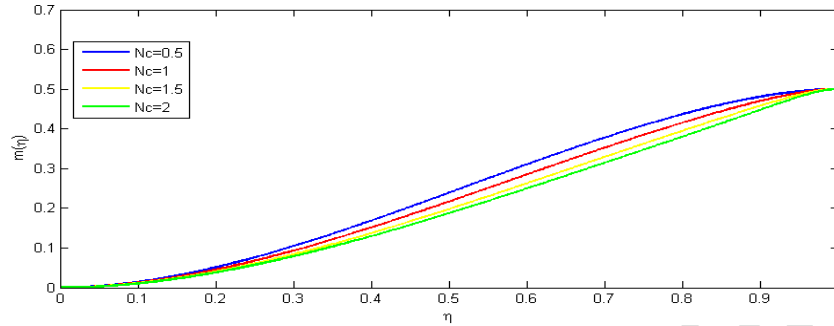


Figure 6a: Shows the graph of  $m'(\eta)$ ,  $m(\eta)$ ,  $n(\eta)$  and  $k(\eta)$  with various values of  $N_c$  and constant values of  $N_b = 0.1, N_d = .5, N_{em} = 3, P_r = .1, H_m = 10, P_m = 1, P_s = 1, m_\eta = .1, E_c = 0.1, N_c = 3$ .

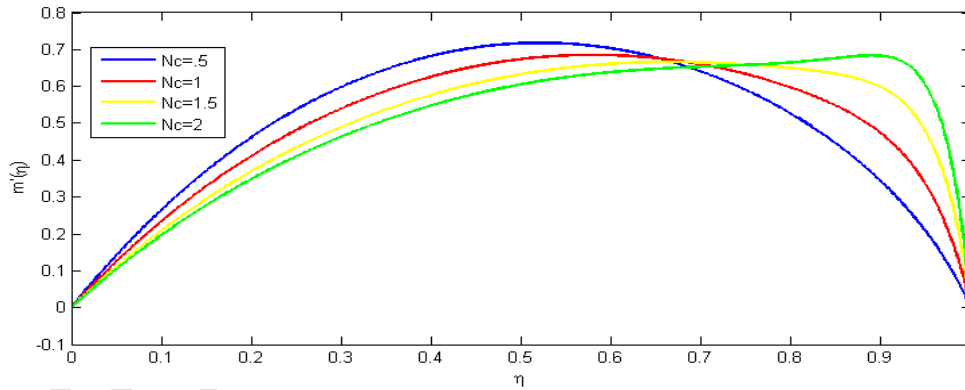


Figure 6b: Shows the graph of  $m'(\eta)$ ,  $m(\eta)$ ,  $n(\eta)$  and  $k(\eta)$  with various values of  $N_c$  and constant values of  $N_b = 0.1, N_d = .5, N_{em} = 3, P_r = .1, H_m = 10, P_m = 1, P_s = 1, m_\eta = .1, E_c = 0.1$ .

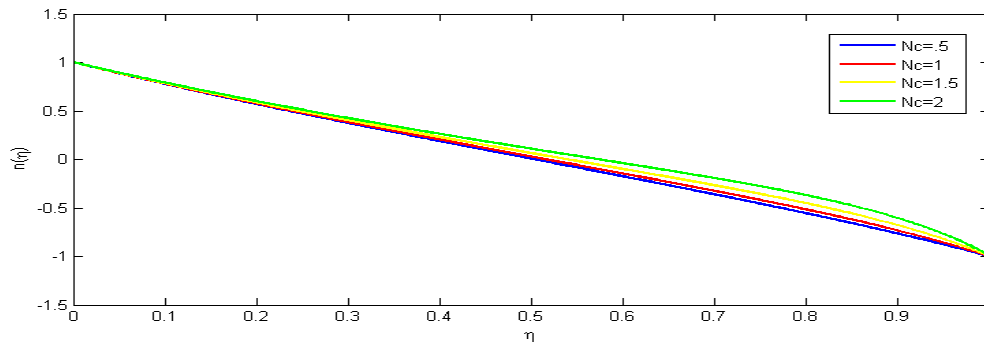


Figure 6c: Shows the graph of  $m'(\eta)$ ,  $m(\eta)$ ,  $n(\eta)$  and  $k(\eta)$  with various values of  $N_c$  and constant values of  $N_b = 0.1, N_d = .5, N_{em} = 3, P_r = .1, H_m = 10, P_m = 1, P_s = 1, m_\eta = .1, E_c = 0.1, N_c$

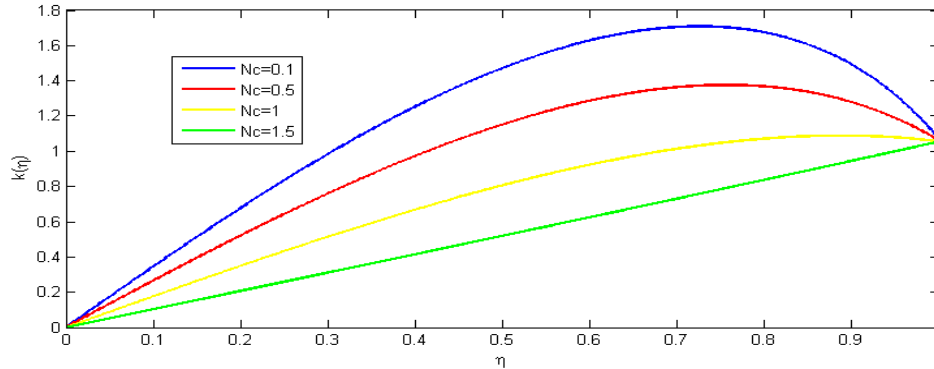


Figure 6d: Shows the graph of  $m'(\eta)$ ,  $m(\eta)$ ,  $n(\eta)$  and  $k(\eta)$  with various values of  $N_c$  and constant values of  $N_b = 0.1, N_d = .5, N_{em} = 3, P_r = .1, H_m = 10, P_m = 1, P_s = 1, m_\eta = .1, E_c = 0.1, N_c = 3$ .

Figure. 6 shows the effect of  $N_c$  on velocity component in y-direction i.e.  $m(\eta)$  and on velocity component in x-direction i.e.  $m'(\eta)$ . As  $N_c$  shows the strength of applied magnetic field in y-direction, so on increasing  $N_c$  the velocity component in x-direction i.e.  $m'(\eta)$  decreases in the surrounding of lower plate while it increases near the region of upper plate in figure 6b. Figure 6a indicates that as the velocity component in y direction i.e.  $m(\eta)$  decreases. Figure 6 (c-d) shows that on increasing  $N_c$  the velocity component in z-direction i.e.  $n(\eta)$  near to upper plate are increasing and it decrease the magnetic component in z-direction i.e.  $k(\eta)$ .

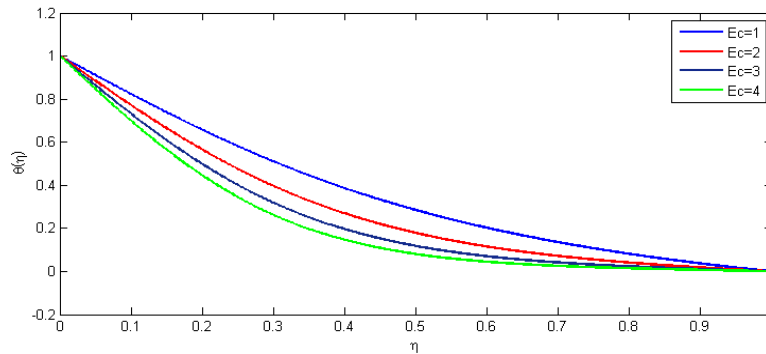


Figure 7a: shows the graph of  $\theta(\eta), \varphi(\eta)$ , with various values of  $E_c$  and constant values of  $N_b = 0.2, N_d = 1, N_{em} = .5, P_r = 10, H_m = 10, P_m = 1, P_s = .5, m_\eta = 2, E_c = 0.1, N_c = 3$ .

The Eckert number  $E_c$  is the ratio of the kinetic energy to the boundary layer enthalpy difference and is used to characterized heat dissipation. Figure 7(a) Shows the increasing  $E_c$  decreasing the  $\theta(\eta)$ , due to temperature difference.

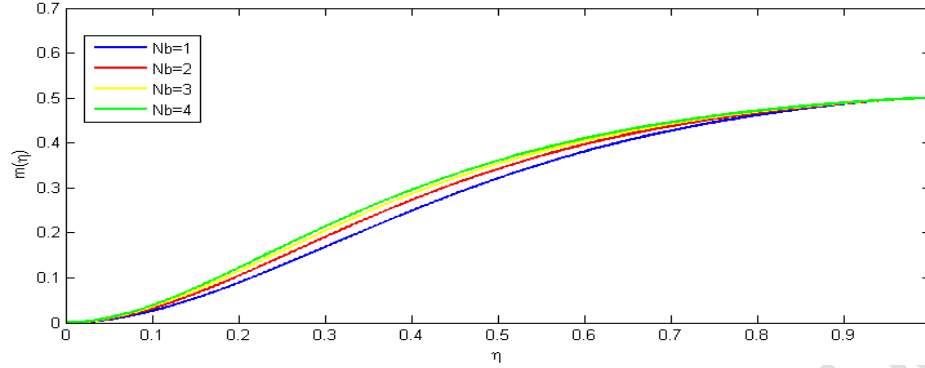


Figure 8a: shows  $m'(\eta)$ ,  $m(\eta)$ ,  $n(\eta)$ ,  $k(\eta)$ , the  $\theta(\eta)$  and  $\varphi(\eta)$  with various values of  $N_b$  and constant values of  $N_c = 8$ ,  $N_d = .1$ ,  $N_{em} = 3$ ,  $P_r = 2$ ,  $H_m = 10$ ,  $P_m = 1$ ,  $P_s = .5$ ,  $m_\eta = .1$ ,  $E_c = 0.1$ .

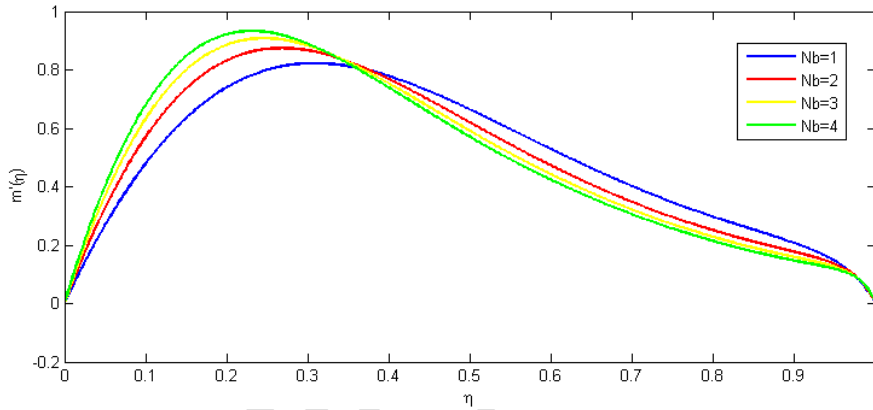


Figure 8b: shows  $m'(\eta)$ ,  $m(\eta)$ ,  $n(\eta)$ ,  $k(\eta)$ , the  $\theta(\eta)$  and  $\varphi(\eta)$  with various values of  $N_b$  and constant values of  $N_c = 8$ ,  $N_d = .1$ ,  $N_{em} = 3$ ,  $P_r = 2$ ,  $H_m = 10$ ,  $P_m = 1$ ,  $P_s = .5$ ,  $m_\eta = .1$ ,  $E_c = 0.1$ .

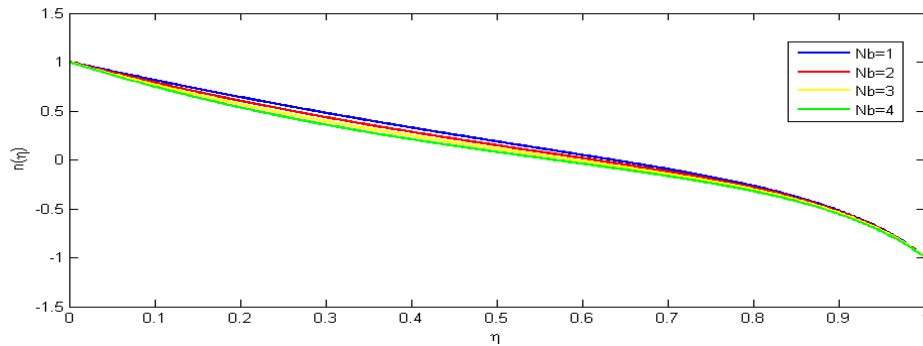


Figure 8c: shows  $m'(\eta)$ ,  $m(\eta)$ ,  $n(\eta)$ ,  $k(\eta)$ , the  $\theta(\eta)$  and  $\varphi(\eta)$  with various values of  $N_b$  and constant values of  $N_c = 8$ ,  $N_d = .1$ ,  $N_{em} = 3$ ,  $P_r = 2$ ,  $H_m = 10$ ,  $P_m = 1$ ,  $P_s = .5$ ,  $m_\eta = .1$ ,  $E_c = 0.1$ .

The squeezing Reynolds number  $N_b$  present the ratio between normal velocity of upper body and kinematic viscosity of the fluid. Figure 8 shows the effect of squeezing Reynolds number on velocity component of  $m(\eta)$  and  $m'(\eta)$ . Figure 8a indicates that as the squeezing Reynold's number increases the velocity component in x-direction decreases in the surrounding of lower plate while it increases near the region of upper plate. Similarly, opposite behavior can be seen in figure 3b where the y-component of velocity

increases. Figure 8c indicate that the squeezing Reynold number increase the velocity component in z direction decrease

Also table2 shows increase in viscosity decrease in skin friction  $m''(0)$  and slightly increase heat flux  $-\theta'(0)$ . Similarly, effect of  $N_{em}$  and  $E_c$  is shown in Table 3-4. Table 5-6 shown the effect of  $P_m$  and  $P_s$  on  $m''$ ,  $n'$ ,  $h'$ ,  $\theta'$  and  $\varphi'$ .

### 3.4 Concluding remark

The mathematical formulation for the constitutive expression, Maxwell equations, energy equation and concentration equation for an unsteady of viscous fluid is employed to model the flow between the two squeezing plates in the form of equations (7) - (12), subject to the boundary conditions given in equation (3.13). Analysis of these equations are performed by PCM and compared with numerical results obtain from BVP4C Package. The following conclusions are drawn with the help of tabulated and graphical results:

- Opposite behavior of the velocity along the x-axis and y-axis with increase in MFD viscosity.
- Magnetic field distribution  $h(\eta)$  decrease with increasing Magnetic Reynold number
- Eckert number have same effect on  $\theta(\eta)$ ,  $\psi(\eta)$ .
- Opposite behavior of X component and y component of velocity with increasing Squeezing Reynold number
- Table 2. show that  $m''(0)$  decrease and increase  $-\theta'$  with increasing MFD viscosity

### References:

- [1] Hathaway, D. B. (1979). Use of ferrofluid in moving-coil loudspeakers. *Db-Sound Engineering Magazine*, 13(2), 42-44.
- [2] MORIMOTO, Y., AKIMOTO, M., & YOTSUMOTO, Y. (1982). Dispersion state of protein-stabilized magnetic emulsions. *Chemical and pharmaceutical bulletin*, 30(8), 3024-3027.
- [3] Soward, A. M. (2002). An Introduction to Magnetohydrodynamics. By PA DAVIDSON. Cambridge University Press, 2001. 431 pp. *Journal of Fluid Mechanics*, 450, 408-410.
- [4] Rashidi, M. M., Rostami, B., Freidoonimehr, N., & Abbasbandy, S. (2014). Free convective heat and mass transfer for MHD fluid flow over a permeable vertical stretching sheet in the presence of the radiation and buoyancy effects. *Ain Shams Engineering Journal*, 5(3), 901-912.
- [5] Khan, A., Shah, R. A., Shuaib, M., & Ali, A. (2018). Fluid dynamics of the magnetic field dependent thermosolutal convection and viscosity between coaxial contracting discs. *Results in Physics*, 9, 923-938.
- [6] Mutua, N. (2013). *Stokes problem of a convective flow past a vertical infinite plate in a rotating system in presence of variable magnetic field* (Doctoral dissertation).
- [7] Seth, M. (2011). The problem considered when the fluid flow is confined to porous boundaries with suction and injection. *Langmuir*, 29(46), 14057-14065.
- [8] Job, V. M., & Gunakala, S. R. (2013). Unsteady mhd free convection Couette flow between two vertical permeable plates in the presence of thermal radiation using galerkin's finite element method. *International Journal of Mechanical Engineering*, 2(5), 99-110.
- [9] Simon, D. (2014). Effect of Heat of Transfer on Unsteady MHD Couette Flow between Two Infinite Parallel Porous Plates in an Inclined Magnetic Field. *Inter. J. Math. Stat. In*, 2(6), 2321-4767.
- [10] Rashidi, M. M., Freidoonimehr, N., Momoniat, E., & Rostami, B. (2015). Study of nonlinear MHD tribological squeeze film at generalized magnetic reynolds numbers using DTM. *PloS one*, 10(8), e0135004.

[11] Shrama, P. R., & Singh, G. (2010). Steady MHD natural convection flow with variable electrical conductivity and heat generation along an isothermal vertical plate. *Journal of Applied Science and Engineering*, 13(3), 235-242.

[12] Hunt, J. C., & Holroyd, R. J. (1977). Applications of laboratory and theoretical MHD duct-flow studies in fusion-reactor technology.

[13] Morley, N. B., Malang, S., & Kirillov, I. (2005). Thermofluid magnetohydrodynamic issues for liquid breeders. *Fusion science and technology*, 47(3), 488-501.

[14] Khan, A., Shah, R. A., Shuaib, M., & Ali, A. (2018). Fluid dynamics of the magnetic field dependent thermosolutal convection and viscosity between coaxial contracting discs. *Results in Physics*, 9, 923-938.

[15] Aly, A. M., & El-Sapa, S. (2021). Double rotations of cylinders on thermosolutal convection of a wavy porous medium inside a cavity mobilized by a nanofluid and impacted by a magnetic field. *International Journal of Numerical Methods for Heat & Fluid Flow*.

[16] Nath, R., & Murugesan, K. (2022). Impact of nanoparticle shape on thermo-solutal buoyancy induced lid-driven-cavity with inclined magnetic-field. *Propulsion and Power Research*, 11(1), 97-117.

[17] Tijani, Y. O., Oloniju, S. D., Kasali, K. B., & Akolade, M. T. (2022). Nonsimilar solution of a boundary layer flow of a Reiner–Philippoff fluid with nonlinear thermal convection. *Heat Transfer*

UNDER PEER REVIEW